Mastocytosis-derived extracellular vesicles exhibit a mast cell signature, transfer KIT to stellate cells, and promote their activation

Do-Kyun Kim[a], Young-Eun Cho[b], Hirsh D. Komarow[a], Geethani Bandara[a], Byoung-Joon Song[b], Ana Olivera[a,1,2], and Dean D. Metcalfe[a,1]

[a]Mast Cell Biology Section, Laboratory of Allergic Diseases, National Institute of Allergy and Infectious Diseases, National Institutes of Health, Bethesda, MD 20892; and [b]Section of Molecular Pharmacology and Toxicology, Laboratory of Membrane Biochemistry and Biophysics, National Institute on Alcohol Abuse and Alcoholism, National Institutes of Health, Bethesda, MD 20892

Edited by Dennis A. Carson, University of California, San Diego, La Jolla, CA, and approved October 1, 2018 (received for review June 13, 2018)

Extracellular vesicles (EVs) have been implicated in the development and progression of hematological malignancies. We thus examined serum samples from patients with systemic mastocytosis (SM) and found EVs with a mast cell signature including the presence of tryptase, FcεRI, MRGX2, and KIT. The concentration of these EVs correlated with parameters of disease including levels of serum tryptase, IL-6, and alkaline phosphatase and physical findings including hepatosplenomegaly. Given reports that EVs from one cell type may influence another cell's behavior, we asked whether SM-EVs might affect hepatic stellate cells (HSCs), based on the abnormal liver pathology associated with mastocytosis. We found that KIT was transferred from SM-EVs into an HSC line eliciting proliferation, cytokine production, and differentiation, processes that have been associated with liver pathology. These effects were reduced by KIT inhibition or neutralization and recapitulated by enforced expression of KIT or constitutively active D816V-KIT, a gain-of-function variant associated with SM. Furthermore, HSCs in liver from mice injected with SM-EVs had increased expression of α-SMA and human KIT, particularly around portal areas, compared with mice injected with EVs from normal individuals, suggesting that SM-EVs can also initiate HSC activation in vivo. Our data are thus consistent with the conclusion that SM-EVs have the potential to influence cells outside the hematological compartment and that therapeutic approaches for treatment of SM may be effective in part through inhibition of effects of EVs on target tissues, findings important both to understanding complex disease pathology and in developing interventional agents for the treatment of hematologic diseases.

extracellular vesicles | systemic mastocytosis | mast cells | liver fibrosis | hepatic stellate cells

Systemic mastocytosis (SM) is a clonal disorder in which there is a pathological accumulation of mast cells in tissues including the bone marrow, skin, lymph nodes, liver, and spleen (1, 2). SM exhibits various degrees of severity, from indolent SM (ISM) to more aggressive forms. Somatic gain-of-function mutations in *KIT*, the cognate receptor for stem cell factor (SCF), especially the c.2447A > T p.(D816V) missense variant, promotes ligand-independent signaling and is associated with the clonal expansion of mast cells in mastocytosis. Disease progression is reflected in a rise in serum levels of mast cell tryptase (3–5), IL-6 (6, 7), and alkaline phosphatase (AP) (8, 9) and is accompanied by progressive hepatosplenomegaly, the latter accompanied by periportal infiltrates and fibrosis (9). Such pathological findings have been attributed to excess mast cell products, although underlying mechanisms are poorly understood (1, 2).

Extracellular vesicles (EVs), such as exosomes (40–150 nm in diameter) and microvesicles (50–1,000 nm in diameter), are released to some degree by most types of cells including mast cells (10, 11), dendritic cells (12, 13), natural killer cells (14), intestinal epithelial cells (15), and B lymphocytes (16). They are also released by cancerous cells including those in hematological malignancies (17, 18), which may generate a greater number of exosomes than normal cells (19, 20). EVs generally contain cell type-specific proteins and nucleic acids (21). It is thought that their distinct traits provide a unique form of cell-to-cell communication by delivering their protected cargoes into bystander cells and altering their responses (19, 22, 23). EVs have thus been reported to affect biological processes such as hematopoietic cell development, immune surveillance, and tissue differentiation and repair (22). In addition, emerging evidence suggests that EVs secreted by transformed cells can stimulate oncogenic reprograming in the tumor environment and promote cancer progression or contribute to pathogenic processes (22, 24). These observations led us to characterize EVs in patients with mastocytosis and probe their biologic function.

As will be shown, mastocytosis-derived EVs (SM-EVs) contain a signature of mast cell-specific proteins, and the concentration of SM-EVs in the serum of patients with mastocytosis correlates with tryptase levels and other markers of disease. Because of the known occurrence of hepatomegaly in patients with mastocytosis associated with periportal infiltrates and fibrosis, we further investigated the effects of SM-EVs on human hepatic stellate cells (HSCs), known to be involved in promoting hepatic injury and fibrosis. We found that KIT contained within SM-EVs is

Significance

Pathological findings in systemic mastocytosis (SM) are generally attributed to an increase in the mast cell burden and associated production of mast cell mediators. We now describe that serum from patients with SM contains extracellular vesicles (EVs) with a mast cell signature and that their concentrations correlate with surrogate markers of disease. These SM-EVs have the ability to alter hepatic stellate cell function including promoting a fibrotic phenotype, partly through the introduction of activated KIT. Tyrosine kinase inhibitors used to treat SM reversed these effects. These observations provide additional insight into how mast cells influence other organ systems in mastocytosis and suggest that targeting the release and/or effects of EVs might be of value in conjunction with existing therapeutic approaches.

Author contributions: D.-K.K., Y.-E.C., and A.O. designed research; D.-K.K. and Y.-E.C. performed research; H.D.K., G.B., and B.-J.S. contributed new reagents/analytic tools; H.K. provided patient samples; A.O. and D.D.M. supervised the study; D.-K.K., Y.-E.C., and A.O. analyzed data; and D.-K.K., B.-J.S., A.O., and D.D.M. wrote the paper.

The authors declare no conflict of interest.

This article is a PNAS Direct Submission.

[1]A.O. and D.D.M. contributed equally to this work.

[2]To whom correspondence should be addressed. Email: ana.olivera@nih.gov.

This article contains supporting information online at www.pnas.org/lookup/suppl/doi:10.1073/pnas.1809938115/-/DCSupplemental.

Published online October 23, 2018.

delivered into HSCs, promoting their proliferation and differentiation into extracellular matrix-producing cells, a characteristic phenotypic change associated with liver pathology.

Results

Clinical Correlations with EV Concentration. Increased numbers of circulating EVs have been found in association with solid tumors and hematological disorders. The latter include acute lymphoblastic, acute myeloid, and chronic lymphocytic leukemias, where EVs have been suggested to contribute to disease pathology by a number of mechanisms (25, 26), including effects on stromal cells (27, 28), myeloid-derived suppressor cells (29), and $CD4^+$ T cells (30). Based on these observations, we sought to characterize EVs associated with mastocytosis and explore their potential to contribute to disease pathology. The characteristics of patients with mastocytosis included in this study are shown in Table 1. They were selected to focus on mast cell-derived EVs and thus did not include patients with an associated hematological neoplasm. All patients had ISM (the most common variant of mastocytosis in adults) by the 2008 WHO criteria (31). Four within the higher tryptase group had smoldering systemic mastocytosis (SSM) when reclassified according to 2017 WHO criteria (32). To simplify further analysis of EV content relating to mast cell burden, patients with SM were divided into two groups: those with tryptase values below and those above the median tryptase level (110 ng/mL) in this cohort. As expected, those in the group with tryptase >110 ng/mL had greater percentages of mast cells in the marrow and were more likely to have documented organomegaly (Table 1) (3–5).

We first isolated and compared EVs using two different techniques as described in *Materials and Methods* and shown in the *SI Appendix*, Fig. S1 *A–C*, where EVs isolated by either method appeared similar and with sizes consistent with exosomes or small EVs. We then determined the number of serum EVs in patients with mastocytosis compared with those in healthy volunteers (HVs) employing nanoparticle tracking analysis (NTA) (*SI Appendix*, Fig. S1 *D* and *E*). As might be expected, the EV concentration in patients with mastocytosis was significantly greater than in control subjects ($P < 0.0001$) (Fig. 1*A* and *SI Appendix*, Fig. S2 *A*, *Left*). Similar results were obtained when the precipitation method for EV isolation was combined with purification columns to eliminate potentially contaminating serum proteins and lipoproteins as described in *Materials and Methods* (ExoQuick-ULTRA and ExoQuick-LP) (*SI Appendix*, Fig. S2*B*). We also found that serum from patients with tryptase >110 ng/mL had significantly higher median EV concentrations than those with tryptase <110 ng/mL (Fig. 1*A* and *SI Appendix*, Fig. S2 *A* and *B*), and actually, the EV concentration in patients with mastocytosis strongly correlated with serum tryptase levels (Fig. 1*B* and *SI Appendix*, Fig. S2 *A*, *Right*) ($P < 0.0029$ and $P < 0.0014$, respectively, for EVs isolated by precipitation and ultracentrifugation).

We next examined the relationships between EV concentration and additional surrogate markers of mastocytosis and aspects of disease pathology. Similar to serum tryptase (Fig. 1*B*), EV concentration positively correlated to IL-6 levels (Fig. 1*C*; $r = 0.6112$, $P = 0.0042$), known to increase with disease severity (6, 7). The concentration of SM-derived EVs also highly correlated with serum levels of AP (Fig. 1*D*; $r = 0.8414$, $P < 0.0001$) and sedimentation rate (Fig. 1*E*; $r = 0.4866$, $P = 0.0296$). Since increased AP in patients with mastocytosis may associate with liver pathology (8) and the presence of hepatomegaly with elevated risk of death (8, 33, 34), we also examined the correlation of EVs in serum with organomegaly. Patients with organomegaly had a significantly higher serum EV concentration than patients without organomegaly (Fig. 1*F*; $P = 0.0386$). As expected, serum tryptase levels also generally correlated with the levels of IL-6 and AP and sedimentation rate as well as organomegaly (*SI Appendix*, Fig. S3 *A–D*). Overall, the EV concentration in mastocytosis correlated with adverse prognostic parameters, as did tryptase (compare Fig. 1 with *SI Appendix*, Fig. S3). These findings are in agreement with reports that more aggressive forms of clonal diseases generate greater amounts of EVs (25) and thus may offer an additional means to assess disease in patients with mastocytosis.

EVs in SM Exhibit a Mast Cell Signature. Since EVs in patients with malignant neoplastic disease in large part originate from cancerous cells (19, 24, 25, 35), we next examined whether EVs from patients with mastocytosis provide evidence of originating from malignant mast cells. We found that EVs isolated from 100 μL of serum from patients with mastocytosis but not those from HV contained KIT, the α and γ subunits of FcεRI, the mas-related G protein-coupled receptor family member X2 (MRGX2), and tryptase, all characteristically expressed by mast cells (36) (Fig. 2*A*). Despite their dense core (*SI Appendix*, Fig. S1*B*) and content of tryptase (Fig. 2*A*), SM-EVs did not present characteristics of secretory granules: They were at least 10-fold smaller (~90 nm; *SI Appendix*, Fig. S1 *D* and *E*) than the average mast cell granule (37), did not contain high levels of histamine or heparin as secretory granules do (*SI Appendix*, Fig. S4 *A*, *Left* and *Middle*), and did not contain prohibitin (*SI Appendix*, Fig. S4 *A*, *Right*), a scaffold protein abundant in mast cell granules (38). Thus, small EVs in the serum of patients with SM contain hallmark proteins characteristic of mast cells but are distinct from secretory granules in size and composition.

Similar protein expression patterns were observed in EVs isolated by ultracentrifugation (*SI Appendix*, Fig. S4*B*) or in EVs from plasma instead of serum (*SI Appendix*, Fig. S4*C*). Also, similar amounts of tryptase were present in EVs when further purification steps were performed (*SI Appendix*, Fig. S4*D*), making it unlikely that the tryptase contents represent remnant contaminants from the serum samples. Furthermore, increased expression of mast cell markers in SM-EVs compared with HV-EVs was also

Table 1. Characteristics and demographics of patients with ISM

Characteristics	Tryptase < 110 ng/mL, $n = 10$	Tryptase > 110 ng/mL, $n = 11$	Total, $n = 21$
Gender, male:female (%:%)	4:6 (40:60)	2:9 (18:82)	6:15 (29:71)
Age, mean (SD)	47.9 (10.5)	47.8 (9.07)	47.9 (9.5)
Tryptase, mean (SD)	48.1 (33.6)	189.7 (82.5)	122.2 (95.7)
Percent Marrow MCs, mean (SD)	15.0 (7.5)	36.0 (19.7)	26.1 (18.3)
D816V-KIT positive, *n* (%)	9 (90)	11 (100)	20 (95)
Organomegaly, *n* (%)	0 (0)	7 (63.6)	7 (33.3)
Osteoporosis/penia, *n* (%)	4 (40.0)	5 (45.4)	9 (42.9)

Patients were initially classified according to 2008 WHO criteria (31). Four patients within the group with tryptase >100 ng/mL met the 2017 WHO criteria for a new variant of SM: SSM (32, 53). The Percent marrow mast cells (MCs) were determined from bone marrow biopsies.

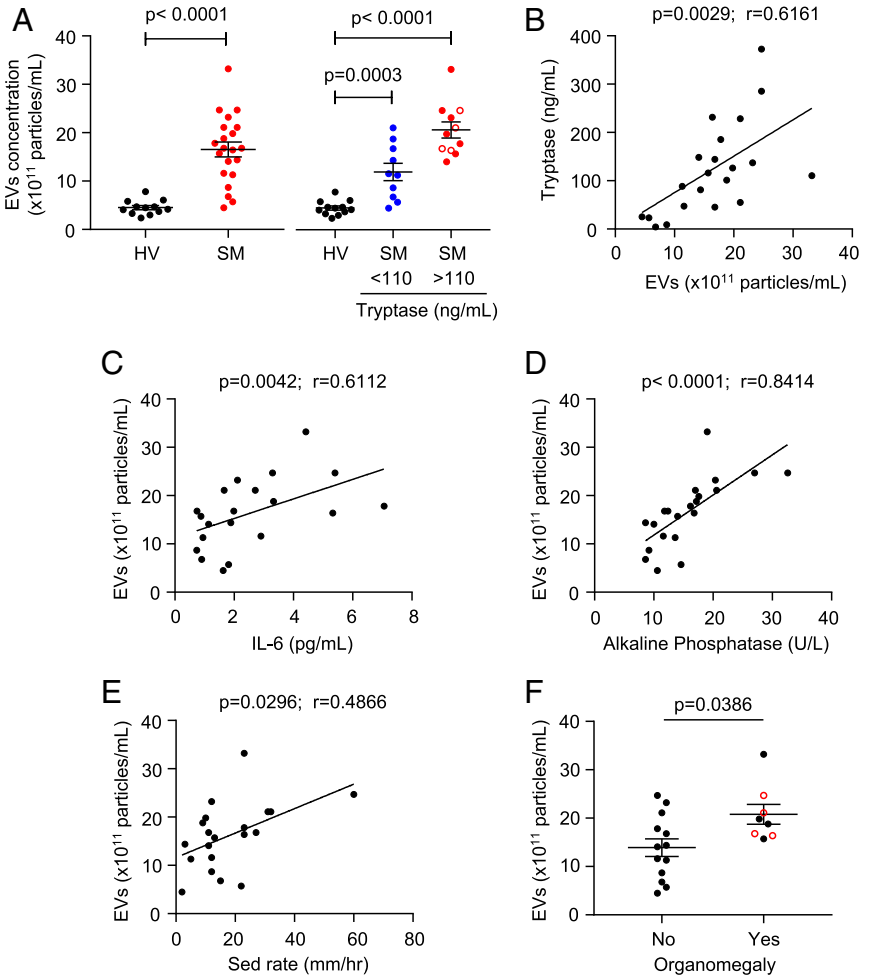

Fig. 1. Concentrations of circulating EVs in patients with SM correlate with parameters of disease severity. (*A*) Quantitative analysis of EV particles in serum from the indicated subject populations. EVs were isolated with ExoQuick solution from the sera of HVs and patients with SM and counted using a NanoSight NS300 system. The SM population was divided into two groups with tryptase values lower or higher than the median (110 ng/mL). Data represent mean ± SEM. (*B–E*) Pearson's correlation between the concentration of EVs in serum and the concentrations of (*B*) tryptase, (*C*) IL-6, (*D*) the activity of AP, and (*E*) sedimentation rate in serum. (*F*) EV concentrations in patients with SM with or without organomegaly. Patients within tryptase >110 ng/mL that met the criteria for SSM (53) are noted as empty red circles.

observed when equal amounts of protein in EV lysates were examined (Fig. 2*B*), demonstrating that the increase in mast cell proteins contained in SM-EVs also reflects differences in composition compared with HV-EVs. Of note, KIT was phosphorylated in SM-derived EVs, consistent with the association of mastocytosis with KIT variants that cause spontaneous activation (and phosphorylation) of this tyrosine kinase receptor. Thus, SM-derived EVs enclose mast cell signature proteins and indicate KIT activation consistent with a neoplastic mast cell origin.

Mastocytosis-Derived EVs Alter HSC Function. Patients with SM over time develop hepatomegaly and elevations in AP. We have reported that liver biopsies performed on patients with SM reveal mast cell infiltration, portal inflammation, portal fibrosis, and venopathy (9). Given the correlations between EV concentration in mastocytosis and AP activity, and sedimentation rate and organomegaly (Fig. 1), we investigated the possibility that SM-EVs could alter the function of HSCs that are involved in hepatic injury and inflammation. HSC activity and numbers are also considered useful in predicting liver fibrosis, and immortalized HSC lines such as LX-2 cells have been developed for studying liver disease in vitro (39–42).

We first questioned whether fluorescently labeled (DiD)-EVs from HV or patients with mastocytosis were effectively taken up by cultured LX-2 cells, generally referred to in this study as HSCs (Fig. 3*A*, red staining). Internalization of labeled EVs could be observed within 2–3 h and was maximal between 12 and 24 h. Cells were also stained with DAPI to label nuclei (Fig. 3*A*, blue staining) and with anti–α-smooth muscle actin (α-SMA), a marker of activation and differentiation of HCS into contractile myofibroblasts (40) (Fig. 3*A*, green staining). The immunocytochemistry confocal images suggested an increase in the number and differentiation of HSCs when treated with SM-derived EVs (note the increased numbers of nuclei per field and increased α-SMA intensity) (Fig. 3*A*). Using a proliferation assay, we then demonstrated that SM-EVs from both groups of patients, particularly in those with tryptase >110 ng/mL, but not HV-EVs, induced proliferation when added to the HSC line for 24 h, an effect that was dependent on the concentration of EVs (Fig. 3*B*). The same increases in proliferation were obtained when cultures were treated with column-purified EVs as described in *Materials and Methods* [proliferation of HSC cells treated with HV-EVs was 109 ± 1.5% of untreated HSCs; with SM-EVs (tryptase < 110 ng/mL), proliferation was 137 ± 2.7%; and with SM-EVs (tryptase > 110 ng/mL), proliferation was 169 ± 3.1%].

To confirm the apparent increase in α-SMA expression observed in the confocal images in Fig. 3*A*, we determined the expression of markers of fibrogenesis by Western blot, including

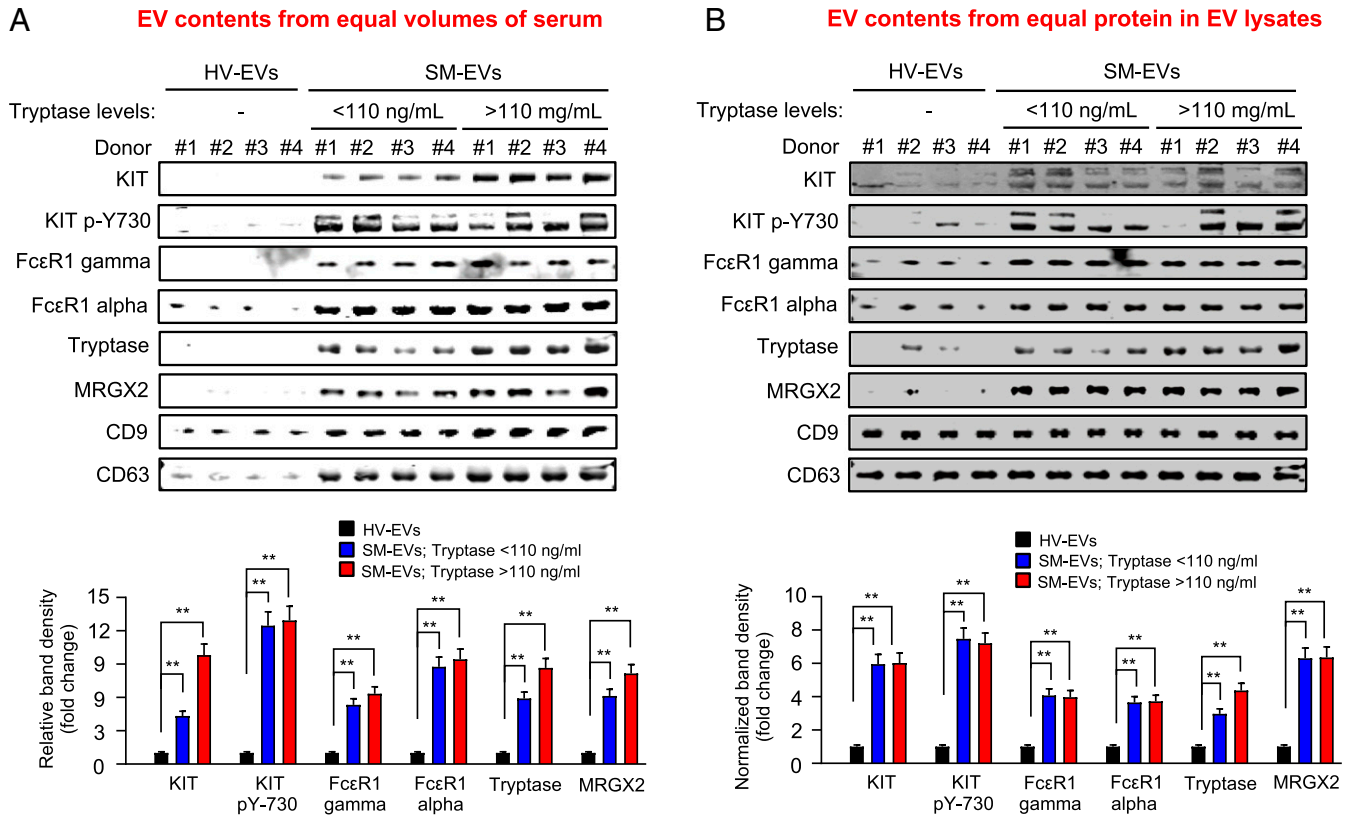

Fig. 2. EVs from patients with SM exhibit a mast cell signature. (*A*) Western blot analysis of EVs isolated from 100 μL of serum from the indicated subjects showing the presence of characteristic receptors for mast cells (KIT, FcεRI-α and -γ subunits, and MRGX2) and mast cell tryptase. Isolated EVs were resuspended in 100 μL of RIPA lysis buffer and equal volumes loaded onto SDS/PAGE gels. CD9 and CD63, common EV markers, are also shown. (*B*) Western blot analysis of EVs lysates where equal total protein amounts were loaded. Protein content in EV lysates was determined using a BCA protein assay. Equal protein content is demonstrated by the similar band intensities of CD9 and CD63. The histograms represent the average band fluorescence intensities within each group (and in *B*, normalized to the average of CD9 and CD63 intensities) and expressed as fold changes compared with the average band intensity in the HV-EV group. Of note, endothelin A and B receptors were not detected in SM-EV. $^{**}P < 0.01$.

α-SMA, extracellular matrix components, and TGF-β. SM-EVs increased the expression of α-SMA, tissue inhibitor of metalloproteinases 1 (TIMP-1), collagen type I, and TGF-β (Fig. 3*C*), consistent with the conclusion that SM-derived EVs induce both the proliferation and differentiation of HSCs into a fibrotic phenotype. We also found that incubation with EVs for 24 h induced the production of proinflammatory cytokines by this HSC line, including IL-6, IL-8, TNF-α, and monocyte chemoattractant protein 1 (MCP-1) (Fig. 3*D*). None of these cytokines were detected in EVs alone in significant levels, indicating the cytokines were produced by HSCs.

To demonstrate that EVs from neoplastic mast cells are sufficient, without contributions from any other cell source, for the phenotypic changes in HSCs, EVs derived from cultures of the mastocytosis cell lines HMC-1.1 and HMC-1.2 were added to HSC cultures. These HMC-1.1– and HMC-1.2–derived EVs (*SI Appendix*, Fig. S5*A*) also enhanced HSC proliferation (*SI Appendix*, Fig. S5*B*) and differentiation (*SI Appendix*, Fig. S5*A*). The effects of SM-EVs appeared to be dependent on the recipient cell type, since SM-EVs, at the same concentrations, did not affect the proliferation of HepG2 cells (*SI Appendix*, Fig. S6*A*), a hepatocellular carcinoma human cell line, or primary murine hepatocytes in culture (*SI Appendix*, Fig. S6*C*), even though SM-EVs were also taken up by these cells (*SI Appendix*, Fig. S6 *B* and *D*).

Active KIT Is Detected in HSC Cultures after Treatment with SM-EVs. A variety of mast cell-related products such as tryptase and receptors expressed in mast cells could be transferred from SM-EVs and cause activation of HSCs (43). Our results revealed that KIT protein expression increased markedly in HSCs (Fig. 4*A* and *SI Appendix*, Fig. S7*A*), while the expression of tryptase was only slightly increased (*SI Appendix*, Fig. S7*A*) after treatment with SM-EVs but not with HV-EVs. In contrast, other SM-EV components such as FcεRI and MRGX2 were not found in HSC lysates after EV treatment (*SI Appendix*, Fig. S7*A*). In addition, the expression of other tyrosine kinase receptors known to affect HSC activation such as VEGFR and PDGFR (39, 40) was either unaltered by incubation with EVs (PDGFR) (Fig. 4*D*) or undetectable (VEGF).

At baseline, HSC cultures barely expressed KIT at the protein or mRNA levels (*SI Appendix*, Fig. S7*B*). The marked increase in KIT expression after incubation with SM-EVs was not due to an induction of KIT transcription in HSCs (*SI Appendix*, Fig. S7*C*), indicating that KIT was transferred from SM-EVs and incorporated into HSCs. Confocal images confirmed that KIT was not expressed in untreated or HV-EV–treated HSCs but was detected in the cell surface and in intracellular locations 6 h after treatment with SM-EVs. However, after 12 h, the location of KIT was primarily intracellular, in perinuclear vesicular structures (*SI Appendix*, Fig. S7*D*) that resembled the endolysosomal vesicle locations described for D816V-KIT (44). The transfer of contents from SM-EVs cannot be generalized to all cell types either, since HepG2 cells, which took up SM-EVs (*SI Appendix*, Fig. S6*B*), did not express KIT (*SI Appendix*, Fig. S6*E*) or phosphorylated KIT. The selective expression of different EV components is consistent with the current view that the mechanisms of EV entry in cells, the fate of EV cargoes, and thus their functional effects vary depending on the recipient cells (45).

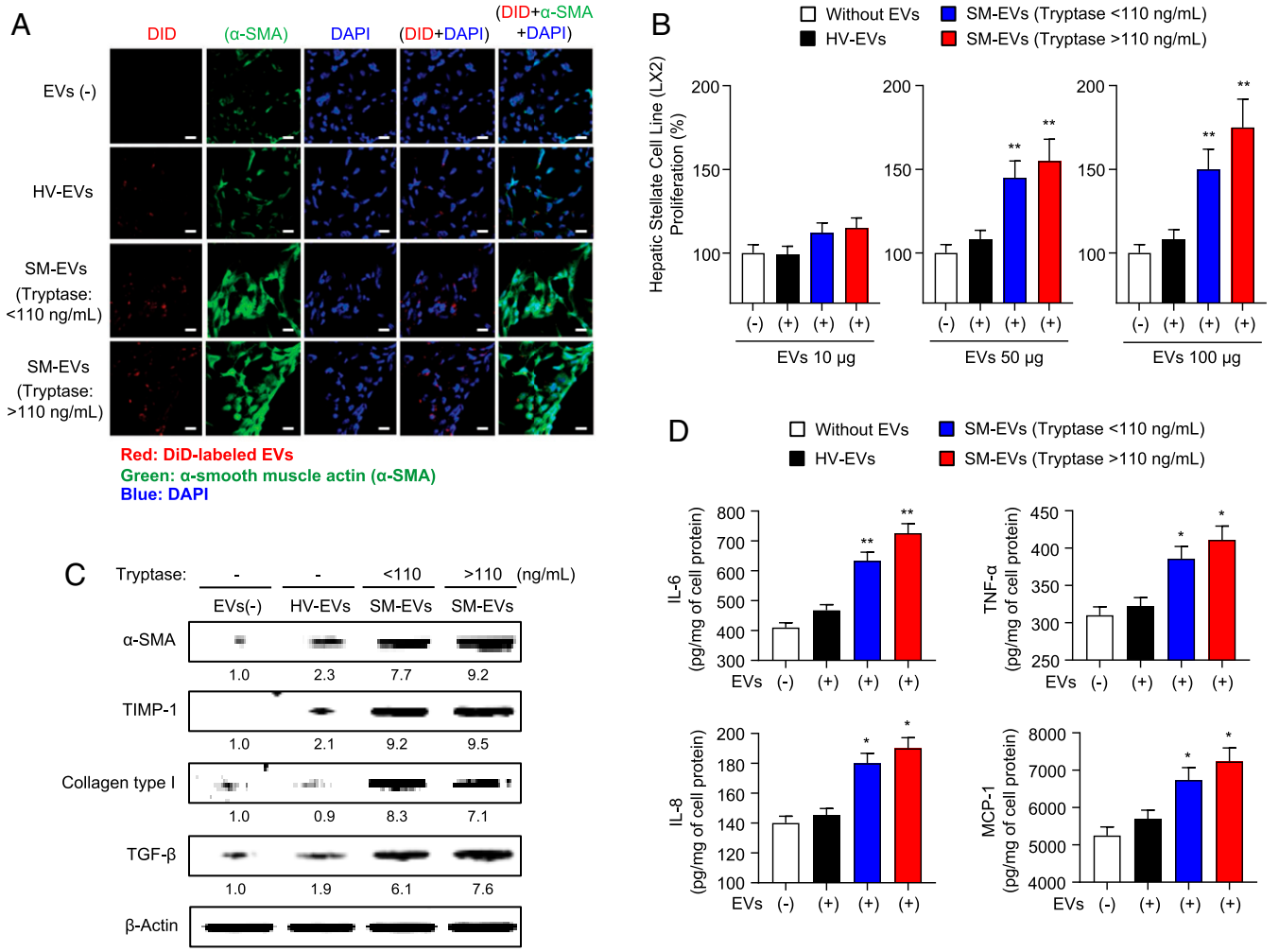

Fig. 3. Serum EVs from patients with SM are taken up by HSCs and promote their activation. EVs from 100 μL of individual serum samples in each group (HV, SM with tryptase <110 ng/mL, and SM with tryptase >110 ng/mL) were pooled together before addition to the cultured stellate cells. (*A*) Confocal images showing uptake of DiD-red fluorescently labeled EVs into HSCs. HSCs were incubated for 24 h with 100 μg DiD-labeled EVs (red) from the indicated groups. Nuclei from cells stained by DAPI are shown in blue and staining of α-SMA, a marker of HSC differentiation, in green. (Scale bar, 50 nm.) (*B*) Proliferation of HSCs in the presence of 10, 50, or 100 μg of EVs isolated from serum from HV or the indicated SM groups. EVs were added to cultured HSCs (in 500 μL of media) in 24-well plates for 24 h. Data represent mean ± SEM of three independent experiments. (*C*) Western blot analysis showing markers of HSC differentiation after 24-h incubation with 100 μg of the indicated EVs. The numbers underneath each band represent the average fold changes in fluorescence intensity normalized to actin and compared with the band intensity of untreated cells. The SD of fold changes for the three experiments was <10% of the mean. (*D*) Effect of SM-EVs on the release of the indicated cytokines by HSCs. HSCs were incubated with 100 μg of EVs of SM-EVs as above for 24 h. Cytokine levels released into the culture media were measured by ELISA, and the quantities released per well were then normalized by the total cellular protein content. $*P < 0.05$, $**P < 0.01$.

An important observation was that KIT expressed in HSC lysates after treatment with SM-EVs was phosphorylated and active, as further demonstrated by tyrosine kinase assays in KIT immunoprecipitates (Fig. 4*A*). To better understand whether the presence of phosphorylated KIT in the HSC line was at least partially ligand-dependent, we explored whether HSCs could release SCF, the ligand for KIT. Indeed, SCF was released constitutively by HSCs treated or not with SM-EVs (*SI Appendix*, Fig. S7*E*), suggesting that KIT transferred from EVs into HSCs could be activated in HSCs in an autocrine manner via the production of SCF or, alternatively, KIT in EVs may be oncogenic and constitutively active due to KIT gain-of function mutations. SCF was, however, not detectable within EVs, indicating HSCs as the source for the ligand.

KIT Inhibition Suppresses SM-EV–Induced Activation of HSCs. As HSC activity may be influenced by tyrosine kinase receptors (39, 40) and KIT was in an active, phosphorylated state in HSCs treated with SM-EVs, we hypothesized that KIT transferred from SM-EVs could mediate the observed phenotypic alterations in these cells. In agreement with this hypothesis, treatment of HSCs with a neutralizing KIT antibody (10 μg/mL) inhibited SM-EV–induced proliferation by 40% (Fig. 4*B*). Although tryptase was also transferred to HSCs from SM-EVs, treatment with tryptase inhibitors known to permeate into cells and to inhibit intracellular proteases had no effect on SM-EV–induced HSC proliferation (*SI Appendix*, Fig. S8 *A*, *Left* and *Middle*). Thus, an intracellular role for tryptase on HSC is unlikely. Furthermore, antagonism of protease activated receptor 2 (PAR2), a receptor previously implicated in liver fibrosis (46), did not reverse the effects of SM-EVs on HSC proliferation (*SI Appendix*, Fig. S8 *A*, *Right*), excluding an involvement of PAR2 if soluble tryptase were to be released from HSC after its incorporation from SM-EVs. Altogether, the results pointed instead toward a role for KIT in SM-EV–induced HSC proliferation.

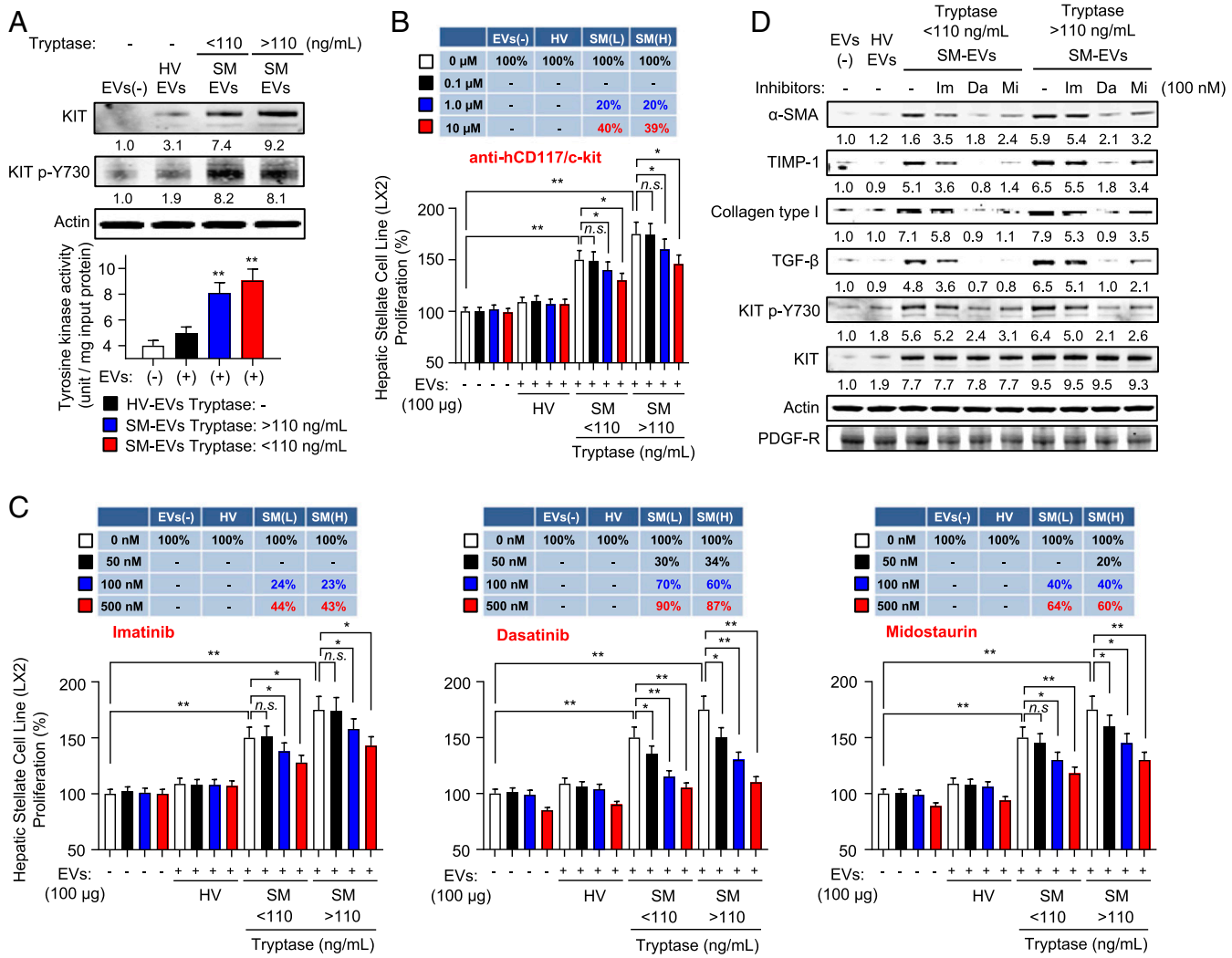

	EVs(-)	HV	SM(L)	SM(H)
0 µM	100%	100%	100%	100%
0.1 µM	-	-	-	-
1.0 µM	-	-	20%	20%
10 µM	-	-	40%	39%

	EVs(-)	HV	SM(L)	SM(H)
0 nM	100%	100%	100%	100%
50 nM	-	-	-	-
100 nM	-	-	24%	23%
500 nM	-	-	44%	43%

	EVs(-)	HV	SM(L)	SM(H)
0 nM	100%	100%	100%	100%
50 nM	-	-	30%	34%
100 nM	-	-	70%	60%
500 nM	-	-	90%	87%

	EVs(-)	HV	SM(L)	SM(H)
0 nM	100%	100%	100%	100%
50 nM	-	-	-	20%
100 nM	-	-	40%	40%
500 nM	-	-	64%	60%

Fig. 4. KIT and its tyrosine kinase activity are increased in HSCs after incubation with SM-EVs, and blockade of KIT prevents SM-EV–induced activation of HSCs. EVs from 100 µL of individual serum samples in each group (HV, SM with tryptase <110 ng/mL, and SM with tryptase >110 ng/mL) were pooled together before their addition to cultured HSCs. (*A*, *Upper*) Western blot analysis of HSC treated with 100 µg of the indicated pooled EVs for 24 h showing SM-EV–dependent enrichment of KIT and phosphorylated KIT in these cells. Cells were thoroughly washed before lysis. (*A*, *Lower*) Increases in KIT activity from HSCs treated with SM-derived EVs. KIT tyrosine kinase activity was determined in immunoprecipitates from HSCs treated or not with different EVs, as indicated. (*B*) Effect of various concentrations of an anti-KIT neutralizing antibody on the proliferation of HSCs treated with 100 µg of HV-EVs or SM-EVs. The antibody was added 20 min before the addition of the EVs and proliferation assessed after 24 h. Data represent mean ± SEM of three independent experiments. (*C*) Proliferation of HSCs in the presence of 100 µg of HV-EVs or SM-EVs treated or not with the tyrosine kinase inhibitors imatinib, dasatinib, and midostaurin at the indicated concentrations. The inhibitors were added 20 min before the addition of exogenous EVs and proliferation assessed after 24 h. The tables above the bar graphs show the percentage inhibition on SM-EV–induced growth increments. Data represent mean ± SEM of three independent experiments. (*D*) Effect of the tyrosine kinase inhibitors on differentiation markers induced by SM-derived EVs in HSCs and on the phosphorylation of KIT. Shown is a representative blot of three individual experiments. The numbers underneath each band in *A* and *D* represent the average fold changes in fluorescence intensity normalized to actin and compared with the band intensity of untreated cells. The SD of fold changes for the three experiments was <10% of the mean. $*P < 0.05$, $**P < 0.01$; n.s., not significant.

We next tested whether inhibition of KIT activity with tyrosine kinase receptor inhibitors commonly used in patients with SM would affect the phenotypic changes in HSCs induced by SM-EVs. Treatment with imatinib, which efficiently inhibits KIT but inefficiently inhibits constitutively active D816V-KIT, caused some inhibition of HSC proliferation (Fig. 4*C*) and differentiation (see α-SMA, TIMP1, collagen type I, and TGF-β expression in Fig. 4*D*) in the presence of SM-EVs. These changes were accompanied by a slight reduction in the phosphorylation of KIT in HSCs (Fig. 4*D*). However, midostaurin and dasatinib, both of which effectively inhibit D816V-KIT, markedly inhibited KIT phosphorylation (Fig. 4*D*) and caused substantial inhibition of HSC proliferation and differentiation even at lower concentrations than imatinib (Fig. 4 *C* and *D*). At 100 nM, dasatinib almost completely inhibited KIT phosphorylation and inhibited HSC proliferation by more than 70%, while at the same concentration, imatinib mildly reduced KIT phosphorylation and only inhibited HSC proliferation by 25% (Fig. 4 *C* and *D*). None of these inhibitors affected EV uptake by HSCs (*SI Appendix*, Fig. S8*B*). Thus, the degree of suppression of KIT phosphorylation by the different inhibitors correlated with their concomitant functional effects on HSC, suggesting a role for EV-transferred KIT, including D816V-KIT, in HSC activation.

As a further proof of concept that KIT can activate HSC, we transfected the HSC line with plasmids encoding for normal KIT (WT-KIT) or D816V-KIT and demonstrated that enforced expression of KIT, particularly D816V-KIT, induced proliferation and differentiation of HSCs in a dose-dependent manner, as did

incubation with SM-EVs (Fig. 5 *A* and *B*). Altogether, the data implicate KIT contained in SM-EVs and transferred to HSCs as a driver of their proliferation and differentiation, although do not exclude potential contributions by other yet unknown EV components.

Treatment of Mice with SM-EVs Results in Uptake of Human KIT and Induction of α-SMA in HSCs. We next investigated the potential for SM-EVs to target HSCs in vivo by injecting SM-EVs or HV-EVs for 3 consecutive days and looking for indications of HSC activation in the liver, such as α-SMA levels (Fig. 6*A*). Western blot analysis of hepatic lysates demonstrated increased expression of α-SMA in recipient mice treated with SM-EVs compared with those treated with HV-EVs (Fig. 6*B*). Furthermore, human KIT was detected in livers of recipient mice treated with SM-EVs (Fig. 6*B*), and as demonstrated by immunoprecipitation of human KIT followed by tyrosine kinase assays, its activity was also increased in mouse livers injected with SM-EVs compared with those treated with HV-EVs (Fig. 6*C*), reminiscent of the correlation found between KIT and α-SMA expression in HSC cultures (Fig. 4).

We then examined the intrahepatic location of α-SMA and KIT by immunohistochemistry. α-SMA expression (red) in livers from all recipient mice was present around portal areas (Fig. 6*D*) but sparse in the liver parenchyma, consistent with the HSC location. Fluorescence intensity staining of α-SMA was greater in livers from mice injected with EVs from patients with ISM or, in this experiment, EVs from patients with SSM (Fig. 6*D*, red staining). Human KIT was also present in association with HSCs and around vessels (Fig. 6*D*, green staining) in what appeared to be cell membrane locations (see arrows to indicate some representative examples) or in intracellular locations. Overall, these data show that HSCs take up KIT from SM-EVs and that SM-EVs induce α-SMA expression in vivo, suggesting a role of KIT within SM-EVs in the activation of HSCs.

Discussion

EVs released by a number of cell types may be enriched in specific proteins and nucleic acids and are thought to play a role in intercellular communication by virtue of the transfer of these materials to recipient cells in adjacent and/or distal sites. Cultured mast cells are known to secrete EVs constitutively or during degranulation (10, 47–49), although their function and significance in vivo are not understood. Here, we report that serum samples of patients with SM contain a high concentration of small EVs with hallmark mast cell proteins and receptors including activated KIT, consistent with the conclusion they originated from clonal mast cells. In addition, we find that the EV concentration in patients with SM correlated with other disease parameters including serum tryptase, a surrogate marker for disease and, when elevated, a minor criterion for diagnosis of mastocytosis. We further provide evidence for a role for SM-derived EVs in the activation of an HSC line, a characteristic implicated in the initiation and development of liver disease, by a mechanism involving incorporation of functionally active KIT from SM-EVs into HSCs. Altogether, the findings (summarized in Fig. 6*E*) indicate that SM-derived EVs are biologically active entities with stroma-modifying activity and the potential of driving some aspects of pathology in mastocytosis.

EV actions may depend on the recipient cell due to differential uptake and fate of SM-EVs in various cell types (i.e., recognition of EVs, trafficking of vesicles and degradation of contents, and the degree of responsiveness of the recipient cell to

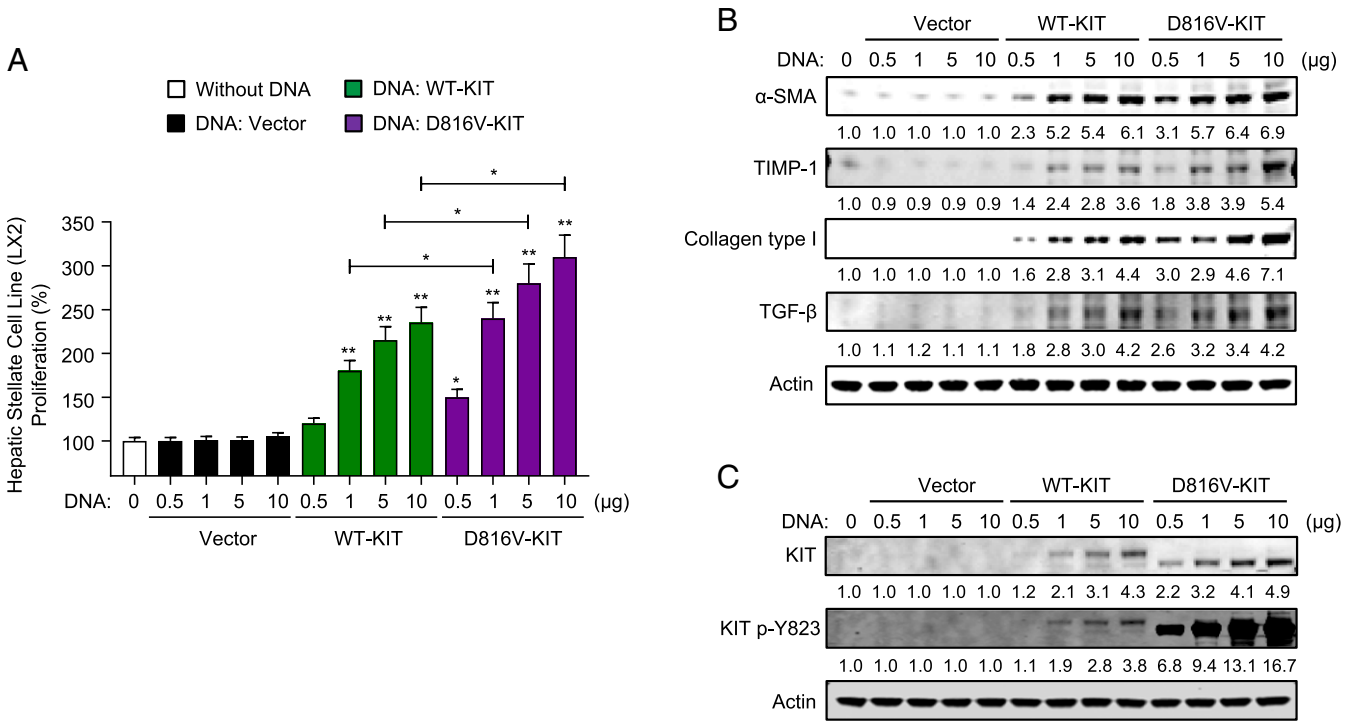

Fig. 5. Enforced expression of WT-*KIT* or D816V-*KIT* induces HSC proliferation and differentiation. (*A*) Proliferation and (*B*) differentiation of HSCs transfected with the indicated amounts of plasmids containing WT-*KIT* or D816V-*KIT*. Two days after transfection, cells were plated in 24-well plates for 24 h. Cell proliferation was measured using an MTT assay (*A*) and changes in markers of differentiation analyzed by Western blots (*B*). Data in *A* are mean ± SEM, and the numbers underneath each band in *B* represent average fold changes in fluorescence intensity normalized to actin and compared with the band intensity of untreated cells ($n = 3$) (SD was <10% of the average). (*A*) $^*P < 0.05$ or $^{**}P < 0.01$, compared with the corresponding vector control or as indicated by the bar. (*C*) Levels of KIT expression and KIT phosphorylation in the same samples are shown for each concentration of plasmid DNA. Note that enforced expression of D816V-KIT results in different mobility in SDS/PAGE, which has been documented in some cells and can be attributed to abnormal glycosylation and/or ubiquitinylation of the mutated receptor (44, 59).

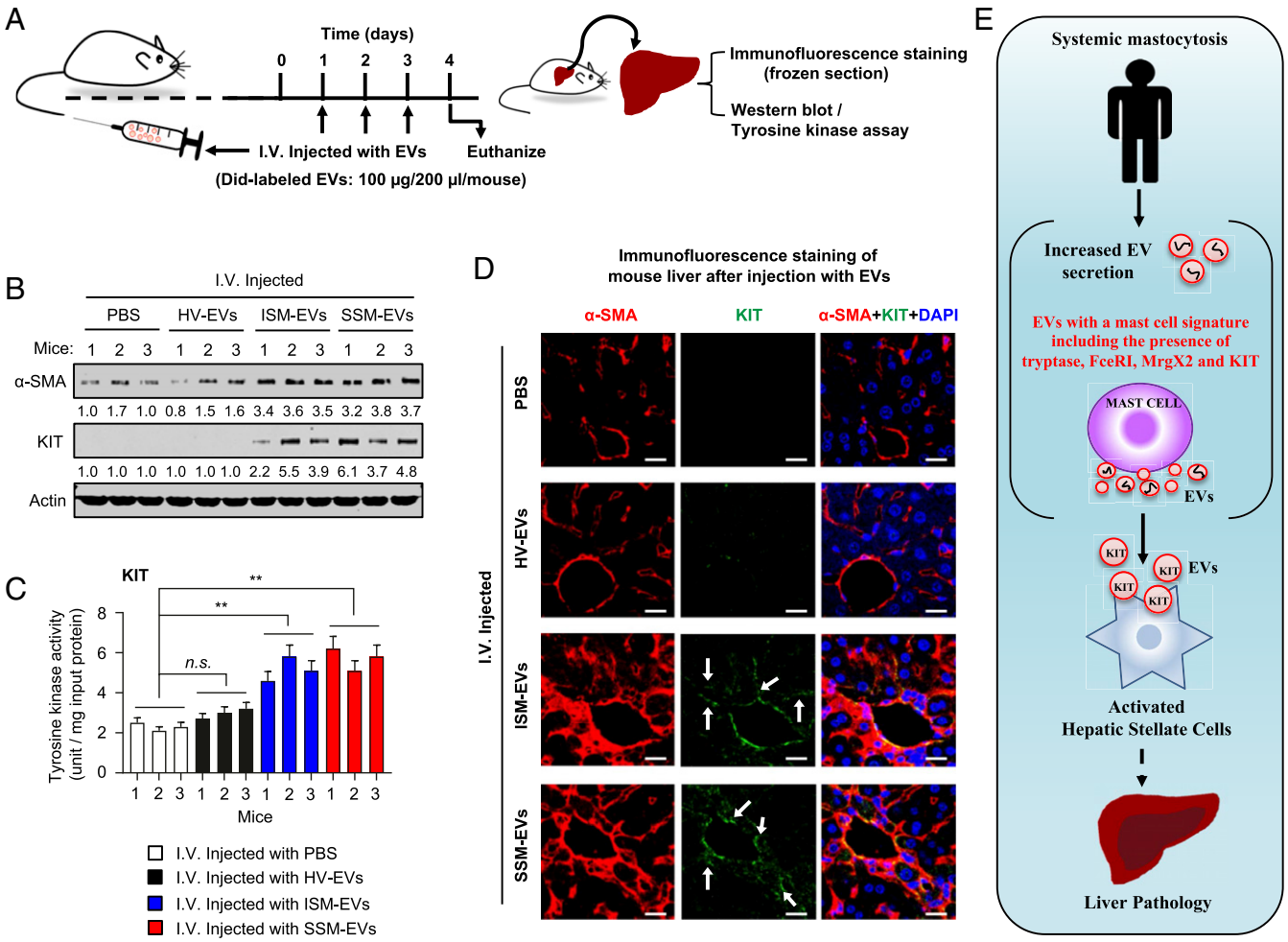

Fig. 6. Human KITs from SM-EVs are taken up by HSCs when injected into mice, and SM-EVs induce activation markers of HSCs. (*A*) Groups of three mice were injected with equal amounts of EVs (100 μg) pooled from four HVs randomly chosen (HV-EVs), a pool of SMs with tryptase<110 ng/mL (four patients) and SMs with tryptase>110 ng/mL (four patients) (ISM-EVs), or a pool of the four patients with SSM (SSM-EVs). (*B*) Liver lysates showing expression of α-SMA and human KIT 24 h after the last injection of the indicated EVs. The numbers underneath each blot in *B* represent average fold changes in fluorescence intensity normalized to actin and compared with the band intensity in mouse 1 of the untreated group. (*C*) Tyrosine kinase activity of KIT in liver lysates was determined following KIT immunoprecipitation. $^{**}P < 0.01$; n.s., not significant. (*D*) Immunostaining of liver sections of recipient mice injected with the indicated types of EVs. Confocal images show staining of α-SMA (red) around hepatic portal areas identifying HSCs and increased intensity of α-SMA staining in recipient mice treated with SM-EVs. Human KIT is shown in green and nuclei from cells in blue following DAPI staining. Arrows indicate examples of seemingly membrane locations. Images were obtained using a 60× objective, and the width of each panel corresponds to 315 μm. (Scale bar, 50 nm.) (*E*) Schematic representation of the data demonstrating increased numbers of circulating EVs with a mast cell signature in patients with SM and their potential contribution to hepatic pathology with HSC proliferation and activation.

cargo molecules) (45). SM-EVs did target HSCs and the EV cargoes induced activation and phenotypic alterations in an HSC line, while neither SM-EVs or P815-derived EVs showed effects on other liver cells such as hepatocytes, despite being taken up by these cells (*SI Appendix*, Fig. S6). HSCs are perisinusoidal cells of mesenchymal origin with central roles in the pathogenesis of liver fibrosis and are considered prognostic indicators of progression of liver fibrosis. Patients with SM tend to develop portal inflammation and fibrosis, and although this correlates with the presence of mast cell infiltrates, the etiology is unknown (9, 50, 51). Various insults activate HSCs to produce extracellular matrix proteins for repair and to promote regeneration of hepatic epithelial cells. However, repeated stimulation of these cells causes a perturbation of liver architecture and function that can lead to increased vascular resistance (39, 40), a pathology that fits the venopathy and occlusion observed in SM (9). In cases of liver fibrosis associated with hepatitis, mast cells are similarly found around portal areas in proximity with HSCs, and a communication between mast cells and HSCs through soluble mediators has been implicated as a mechanism driving liver fibrosis (43, 52). Based on our studies on the LX-2 stellate cell line, we propose yet another mechanism involving EVs by which mast cells may communicate with HSCs and affect their function. In addition to demonstrating that SM-EVs induce HSCs to proliferate, differentiate into fiber-producing cells, and release cytokines in culture, our data show that treatment of mice with SM-EVs caused phenotypic changes in liver consistent with HSC activation in hepatic portal areas, as indicated by increased expression of α-SMA. Our data do not exclude, however, the possibility that the effect of SM-EVs on HSCs in vivo may also be indirect, involving other liver cell types such as Kupffer cells or sinusoidal epithelial cells.

We present evidence that KIT contained in SM-derived EVs is transferred and incorporated into HSCs and plays a major role in inducing HSC proliferation and differentiation: We found that KIT protein, but not its message, was increased in HSCs after

treatment with SM-derived EVs, while other tyrosine kinase receptors such as PDGFR and VEGFR reported to have a function in HSC activation were not increased. Second, KIT was phosphorylated and active in HSCs after incubation with SM-EVs (Fig. 4*A*), and the extent of KIT phosphorylation (Fig. 4*D*) correlated with HSC proliferation (Fig. 4*C*) and differentiation (Fig. 4*D*). These observations led us to question whether inhibitors of KIT employed in the treatment of mastocytosis including dasatinib and midostaurin would inhibit the phenotype induced by SM-derived EVs and found this to be the case (Fig. 4*C*). In addition, treatment with a neutralizing KIT antibody partially inhibited the effect of SM-EVs on HSCs (Fig. 4*B*), consistent with the temporary presence of KIT at the cell surface (*SI Appendix*, Fig. S7*D*), and transfection of HSCs with *KIT* and D816V-*KIT* constructs reproduced the effects induced by SM-EVs in HSCs, demonstrating that KIT can drive this phenotypic change. Lastly, we demonstrated the presence of human KIT in HSCs and increased KIT activity in the livers of recipient mice injected with SM-EV in correlation with enhanced α-SMA expression. We surmise that part of the activity of KIT may be ligand independent due to some presence of active oncogenic KIT in EVs, but when incorporated into HSCs, KIT may also be activated with SCF produced by HSCs. Our results thus indicate that cells other than neoplastic mast cells may acquire a functional pathological outcome by incorporating some neoplastic traits through EVs. The findings support an additional mechanism by which these tyrosine kinase inhibitors act to decrease the pathology associated with mastocytosis.

In summary, we report that EVs shed from human neoplastic mast cells exhibit a mast cell signature profile, that their concentrations in serum correlate with other parameters of disease, and that their cargos can be shuttled into HSCs and dysregulate their function (Fig. 6*E*). The findings, we suggest, have relevance in the understanding of the pathology of liver disease in mastocytosis and suggest that a therapeutic approach targeting EV release and/or uptake might be of therapeutic benefit.

Materials and Methods

Further details can be found in *SI Appendix*.

Subjects. Twenty-one adult patients with ISM, diagnosed in 2015 or earlier in accordance with WHO 2008 guidelines (31), and 12 adult HVs were enrolled and consented on protocols 02-I-0277 and 09-I-0049 approved by the National Institute of Allergy and Infectious Diseases (NIAID, NIH) Institutional Review Board. Updated WHO classifications define a new category of SM, SSM, that was previously included within patients with ISM (32). These patients have less favorable prognosis than those in ISM but more favorable prognosis than in patients with aggressive SM (53). Our cohort contained four patients with SSM who are included within the group of SM with tryptase >110 ng/mL (the median tryptase value in this cohort) (Table 1), since this was their original classification. In some figures, these patients are indicated to be distinguished from others within the ISM category. HVs (5 female and 7 male) ranged in age from 12 to 64 y old (mean age of 40) (Table 1).

Circulating EV Isolation and Characterization. EVs from individual serum samples (100 μL) were purified using ExoQuick solution (54, 55) (System Bioscience) according to the manufacturer's instructions. ExoQuick-ULTRA and ExoQuick-LP methods, which combine precipitation with ExoQuick solution with columns that bind serum proteins (ULTRA) or lipoproteins (LP), were used as directed by the manufacturer to obtain further enriched preparations of EVs. These methods were also used to confirm most of the results using ExoQuick-prepared EVs. Alternatively, EVs were isolated by ultracentrifugation as described (56) and detailed in *SI Appendix* (also see *SI Appendix*, Fig. S1*A*). Briefly, serum samples were clarified by centrifugation at 13,000 × *g* for 40 min at 4 °C and subjected to ultracentrifugation at 120,000 × *g* for 80 min at 4 °C. Pellets were washed, recentrifuged and resuspended in 100 μL PBS.

Electron microscopy of EVs prepared using ExoQuick revealed characteristic EV structures no different from those observed by ultracentrifugation, with cores that appeared denser in SM-derived EVs (*SI Appendix*, Fig. S1*B*). Comparison of EV markers (57) by Western blots (as explained in the *SI Appendix*) of the EV preparations obtained by either precipitation or ultracentrifugation showed similar levels of CD9 and CD63 regardless of the isolation technique, and their expression was uniform between HV- and SM-derived EVs (*SI Appendix*, Fig. S1*C*). In addition, the average EV size and size distribution, as determined by NTA using a NanoSight NS300 system (58) (NanoSight), were similar and consistent with the size of exosomes (50–150 nm) independently of the isolation technique and the origin of the sample (*SI Appendix*, Fig. S1 *D* and *E*). Of note, ∼91% of particles were between 50 and 200 nm, and <2% of particles had sizes >200 nm, suggesting a relatively homogenous population of small EVs. Given the similar purity and quality of serum-derived EVs isolated either by immunoprecipitation or by ultracentrifugation, studies were subsequently performed with EV isolated by precipitation unless otherwise indicated.

Western Blotting. For immunoblot analyses of EV contents, EV preparations were lysed in 100 μL of RIPA buffer as described in *SI Appendix*. EV lysates were kept on ice for 10 min, dissolved in 3× Laemmli buffer before loading into SDS/PAGE gels, and then transferred onto nitrocellulose membranes. Protein determinations in EV lysates were performed using a BCA protein assay (Pierce-ThermoFisher Scientific).

Immunoblot analyses of HSCs treated with EVs were performed as described in *SI Appendix*. For immunoblot analyses of livers of recipient mice injected with exogenous EVs, a liver fragment was excised and placed in RIPA buffer at 4 °C, homogenized using a Dounce homogenizer, and centrifuged at 250 × *g* for 10 min. Equal amounts of proteins in the supernatant (20 μg) were solubilized in 3× SDS sample buffer and loaded onto SDS/PAGE gels.

Cell Proliferation Assays in HSCs and Release of Cytokines, Chemokines, and Growth Factors. The proliferation rate of cultured cells was assessed using the 3-[4,5-dimethylthiazol-2-yl]-2,5-diphenyltetrazolium bromide (MTT) reduction assay (Sigma-Aldrich). The LX-2 human HSC line, the human hepatoma cell line HepG2, and primary mouse hepatocytes were cultured in 24-well plates (8×10^4 cells per well) and maintained in growth media for 24 h at 37 °C under 5% CO_2. At 80% confluency, cells were treated with the indicated concentration of EVs (10 μg, 50 μg, or 100 μg) or carrier control (PBS) for 24 h. When inhibitors were used, these were added at the indicated concentrations 20 min before the addition of EVs. MTT solution (20 μL) was added to each well and incubated at 37 °C for 3 h to allow the production of formazan crystals. The supernatant was removed, and filtered DMSO (200 μL) was added to each well to dissolve the crystals. Absorbance at 570 nm of each well was determined with a microplate reader.

The cytokines, chemokines, and the growth factor SCF released by HSCs after treatment with EVs for 24 h under the experimental conditions described above were measured using ELISA kits for each product (R&D Systems). Cells from each well were lysed as described in the Western blotting section and protein measured using a Bradford assay. The quantities of cytokines released per milligram of cellular protein were then calculated.

Uptake of Labeled EVs in Cell Cultures. EVs were labeled using DiD red-fluorescent dye (ThermoFisher Scientific) at a 1:200 dilution for 10 min following the manufacturer's instructions. DiD dye-labeled EVs were resuspended in PBS and added to cultured cells for 24 h at 37 °C. Cells were then washed twice with PBS, fixed with 4% formaldehyde in PBS for 15 min at room temperature, mounted with ProLong Antifade Kit mounting solution (Molecular Probes), and observed under a confocal microscope (Zeiss).

Treatment of Mice with EVs. Protocols with live mice were approved by NIH/NIAID Animal Care and Use Committee (animal study proposal LAD2E) and were performed in accordance with the Office of Animal Care and Use guidelines. EVs obtained using ExoQuick-ULTRA were DiD-labeled and injected into C57/BL6 mice (8 wk old) via the tail vein once a day for 3 consecutive days (100 μg of EVs in 200 μL of sterile PBS per mouse per day). Pools of EVs isolated from four randomly selected HVs, eight patients with SM (four with tryptase <110 ng/mL and four with tryptase <110 ng/mL), and four patients with SSM were injected, respectively, into three mice for each category of EVs. Mice were euthanized 24 h after the last injection. A fragment of the liver was placed in RIPA buffer for Western blot analysis, and the rest fixed in 10% formalin for 6 h. Subsequently, the livers were placed in 20% sucrose in PBS at 4 °C overnight. Livers were embedded in Tissue Tek OCT compound (Sakura Finetek, Zoeterwoude), dropped in liquid nitrogen for a brief period of time, and stored at −80 °C. Histological specimen slides were blocked with 3% BSA in PBS for 30 min or 1 h and incubated with anti–α-SMA (1:200 dilution; Sigma-Aldrich) and anti-human KIT (1:200 dilution; Invitrogen) antibodies at 4 °C overnight in 1% BSA–PBS.

After extensive washing, Alexa Fluor 594-conjugated goat anti-mouse IgG (Invitrogen) was used to detect α-SMA (red) (1:5,000 dilution) and Alexa Fluor 488-conjugated Donkey anti-Rabbit IgG (Invitrogen) to detect human KIT (green) (1:5,000 dilution). DAPI was also used for nuclear staining. Images (60×) were obtained with a confocal LSM 780 Zeiss microscope.

Statistical Analysis. One-way ANOVA was used to determine statistically significant differences between groups and Pearson's correlation analysis to determine statistically significant associations between parameters. All analyses were performed using Prism 7 software (Graph Pad Software). Statistical significance was indicated as follows: $*P < 0.05$, $**P < 0.01$.

ACKNOWLEDGMENTS. We thank Yun Bai and Pahul Hanjra for help with the patient repository. This research was supported by the Divisions of Intramural Research within NIAID and National Institute on Alcohol Abuse and Alcoholism.

1. Akin C, Valent P (2014) Diagnostic criteria and classification of mastocytosis in 2014. *Immunol Allergy Clin North Am* 34:207–218.
2. Carter MC, Metcalfe DD, Komarow HD (2014) Mastocytosis. *Immunol Allergy Clin North Am* 34:181–196.
3. Sperr WR, et al. (2002) Serum tryptase levels in patients with mastocytosis: Correlation with mast cell burden and implication for defining the category of disease. *Int Arch Allergy Immunol* 128:136–141.
4. Valent P, et al. (2014) The serum tryptase test: An emerging robust biomarker in clinical hematology. *Expert Rev Hematol* 7:683–690.
5. Vitte J (2015) Human mast cell tryptase in biology and medicine. *Mol Immunol* 63:18–24.
6. Brockow K, Akin C, Huber M, Metcalfe DD (2005) IL-6 levels predict disease variant and extent of organ involvement in patients with mastocytosis. *Clin Immunol* 115: 216–223.
7. Mayado A, et al. (2016) Increased IL6 plasma levels in indolent systemic mastocytosis patients are associated with high risk of disease progression. *Leukemia* 30:124–130.
8. Jawhar M, et al. (2016) Splenomegaly, elevated alkaline phosphatase and mutations in the SRSF2/ASXL1/RUNX1 gene panel are strong adverse prognostic markers in patients with systemic mastocytosis. *Leukemia* 30:2342–2350.
9. Mican JM, et al. (1995) Hepatic involvement in mastocytosis: Clinicopathologic correlations in 41 cases. *Hepatology* 22:1163–1170.
10. Groot Kormelink T, et al. (2016) Mast cell degranulation is accompanied by the release of a selective subset of extracellular vesicles that contain mast cell-specific proteases. *J Immunol* 197:3382–3392.
11. Raposo G, et al. (1997) Accumulation of major histocompatibility complex class II molecules in mast cell secretory granules and their release upon degranulation. *Mol Biol Cell* 8:2631–2645.
12. Nolte-'t Hoen EN, Buschow SI, Anderton SM, Stoorvogel W, Wauben MH (2009) Activated T cells recruit exosomes secreted by dendritic cells via LFA-1. *Blood* 113:1977–1981.
13. Zitvogel L, et al. (1998) Eradication of established murine tumors using a novel cell-free vaccine: Dendritic cell-derived exosomes. *Nat Med* 4:594–600.
14. Fais S (2013) NK cell-released exosomes: Natural nanobullets against tumors. *OncoImmunology* 2:e22337.
15. Büning J, et al. (2008) Multivesicular bodies in intestinal epithelial cells: Responsible for MHC class II-restricted antigen processing and origin of exosomes. *Immunology* 125:510–521.
16. Raposo G, et al. (1996) B lymphocytes secrete antigen-presenting vesicles. *J Exp Med* 183:1161–1172.
17. Hood JL, San RS, Wickline SA (2011) Exosomes released by melanoma cells prepare sentinel lymph nodes for tumor metastasis. *Cancer Res* 71:3792–3801.
18. Friel AM, Corcoran C, Crown J, O'Driscoll L (2010) Relevance of circulating tumor cells, extracellular nucleic acids, and exosomes in breast cancer. *Breast Cancer Res Treat* 123:613–625.
19. Antonyak MA, Cerione RA (2015) Emerging picture of the distinct traits and functions of microvesicles and exosomes. *Proc Natl Acad Sci USA* 112:3589–3590.
20. Kalluri R (2016) The biology and function of exosomes in cancer. *J Clin Invest* 126: 1208–1215.
21. Valadi H, et al. (2007) Exosome-mediated transfer of mRNAs and microRNAs is a novel mechanism of genetic exchange between cells. *Nat Cell Biol* 9:654–659.
22. Lo Cicero A, Stahl PD, Raposo G (2015) Extracellular vesicles shuffling intercellular messages: For good or for bad. *Curr Opin Cell Biol* 35:69–77.
23. EL Andaloussi S, Mäger I, Breakefield XO, Wood MJ (2013) Extracellular vesicles: Biology and emerging therapeutic opportunities. *Nat Rev Drug Discov* 12:347–357.
24. Wendler F, et al. (2017) Extracellular vesicles swarm the cancer microenvironment: From tumor-stroma communication to drug intervention. *Oncogene* 36:877–884.
25. Boyiadzis M, Whiteside TL (2017) The emerging roles of tumor-derived exosomes in hematological malignancies. *Leukemia* 31:1259–1268.
26. Prieto D, et al. (2017) S100-A9 protein in exosomes from chronic lymphocytic leukemia cells promotes NF-κB activity during disease progression. *Blood* 130:777–788.
27. Johnson SM, et al. (2016) Metabolic reprogramming of bone marrow stromal cells by leukemic extracellular vesicles in acute lymphoblastic leukemia. *Blood* 128:453–456.
28. Paggetti J, et al. (2015) Exosomes released by chronic lymphocytic leukemia cells induce the transition of stromal cells into cancer-associated fibroblasts. *Blood* 126: 1106–1117.
29. Pyzer AR, et al. (2017) MUC1-mediated induction of myeloid-derived suppressor cells in patients with acute myeloid leukemia. *Blood* 129:1791–1801.
30. Smallwood DT, et al. (2016) Extracellular vesicles released by CD40/IL-4-stimulated CLL cells confer altered functional properties to CD4+ T cells. *Blood* 128:542–552.
31. Horny HP, et al. (2008) Mastocytosis. *WHO Classification of Tumours of Haematopoietic and Lymphoid Tissues*, eds Swerdlow SH, et al. (International Agency for Research on Cancer Press, Lyon, France), pp 54–63.
32. Horny HP, et al. (2017) Mastocytosis. *WHO Classification of Tumours of Haematopoietic and Lymphoid Tissues*, eds Swerdlow SH, et al. (International Agency for Research on Cancer Press, Lyon, France), pp 62–69.
33. Lawrence JB, et al. (1991) Hematologic manifestations of systemic mast cell disease: A prospective study of laboratory and morphologic features and their relation to prognosis. *Am J Med* 91:612–624.
34. Travis WD, Li CY, Bergstralh EJ, Yam LT, Swee RG (1988) Systemic mast cell disease. Analysis of 58 cases and literature review. *Medicine (Baltimore)* 67:345–368.
35. Yeh YY, et al. (2015) Characterization of CLL exosomes reveals a distinct microRNA signature and enhanced secretion by activation of BCR signaling. *Blood* 125:3297–3305.
36. Dwyer DF, Barrett NA, Austen KF; Immunological Genome Project Consortium (2016) Expression profiling of constitutive mast cells reveals a unique identity within the immune system. *Nat Immunol* 17:878–887.
37. Azouz NP, Hammel I, Sagi-Eisenberg R (2014) Characterization of mast cell secretory granules and their cell biology. *DNA Cell Biol* 33:647–651.
38. Kim DK, et al. (2013) The scaffold protein prohibitin is required for antigen-stimulated signaling in mast cells. *Sci Signal* 6:ra80.
39. Yin C, Evason KJ, Asahina K, Stainier DY (2013) Hepatic stellate cells in liver development, regeneration, and cancer. *J Clin Invest* 123:1902–1910.
40. Moreira RK (2007) Hepatic stellate cells and liver fibrosis. *Arch Pathol Lab Med* 131: 1728–1734.
41. Friedman SL (2008) Hepatic stellate cells: Protean, multifunctional, and enigmatic cells of the liver. *Physiol Rev* 88:125–172.
42. Xu L, et al. (2005) Human hepatic stellate cell lines, LX-1 and LX-2: New tools for analysis of hepatic fibrosis. *Gut* 54:142–151.
43. Francis H, Meininger CJ (2010) A review of mast cells and liver disease: What have we learned? *Dig Liver Dis* 42:529–536.
44. Obata Y, et al. (2014) Oncogenic Kit signals on endolysosomes and endoplasmic reticulum are essential for neoplastic mast cell proliferation. *Nat Commun* 5:5715.
45. Abels ER, Breakefield XO (2016) Introduction to extracellular vesicles: Biogenesis, RNA cargo selection, content, release, and uptake. *Cell Mol Neurobiol* 36:301–312.
46. Shearer AM, et al. (2016) Targeting liver fibrosis with a cell-penetrating protease-activated Receptor-2 (PAR2) pepducin. *J Biol Chem* 291:23188–23198.
47. Admyre C, et al. (2008) Exosomes–nanovesicles with possible roles in allergic inflammation. *Allergy* 63:404–408.
48. Skokos D, et al. (2003) Mast cell-derived exosomes induce phenotypic and functional maturation of dendritic cells and elicit specific immune responses in vivo. *J Immunol* 170:3037–3045.
49. Skokos D, Goubran-Botros H, Roa M, Mécheri S (2002) Immunoregulatory properties of mast cell-derived exosomes. *Mol Immunol* 38:1359–1362.
50. Adolf S, et al. (2012) Systemic mastocytosis: A rare case of increased liver stiffness. *Case Rep Hepatol* 2012:728172.
51. Zhang XY, Zhang WH (2014) An unusual case of aggressive systemic mastocytosis mimicking hepatic cirrhosis. *Cancer Biol Med* 11:134–138.
52. Jones H, et al. (2016) Inhibition of mast cell-secreted histamine decreases biliary proliferation and fibrosis in primary sclerosing cholangitis Mdr2(-/-) mice. *Hepatology* 64:1202–1216.
53. Valent P, Akin C, Metcalfe DD (2017) Mastocytosis: 2016 updated WHO classification and novel emerging treatment concepts. *Blood* 129:1420–1427.
54. Manier S, et al. (2017) Prognostic role of circulating exosomal miRNAs in multiple myeloma. *Blood* 129:2429–2436.
55. Njock MS, et al. (2015) Endothelial cells suppress monocyte activation through secretion of extracellular vesicles containing antiinflammatory microRNAs. *Blood* 125: 3202–3212.
56. Chevillet JR, et al. (2014) Quantitative and stoichiometric analysis of the microRNA content of exosomes. *Proc Natl Acad Sci USA* 111:14888–14893.
57. Lee Y, El Andaloussi S, Wood MJ (2012) Exosomes and microvesicles: Extracellular vesicles for genetic information transfer and gene therapy. *Hum Mol Genet* 21: R125–R134.
58. Gercel-Taylor C, Atay S, Tullis RH, Kesimer M, Taylor DD (2012) Nanoparticle analysis of circulating cell-derived vesicles in ovarian cancer patients. *Anal Biochem* 428:44–53.
59. Shi X, et al. (2016) Distinct cellular properties of oncogenic KIT receptor tyrosine kinase mutants enable alternative courses of cancer cell inhibition. *Proc Natl Acad Sci USA* 113:E4784–E4793.